




A Thoroughgoing Study on Engineering Properties of High Strength Concrete at Elevated Temperatures

Ramezan Ali Izadifard, Amir Khalighi, Mehrdad Abdi Moghadam * and Hossein Balouei Pirnaeimi, Department of Civil Engineering, Imam Khomeini International University, Qazvin, Iran

Received: 4 August 2020/**Accepted:** 11 January 2021/**Published online:** 12 February 2021

Abstract. Using high strength concrete, instead of the conventional one, has been increasingly growing in popularity over recent years. However, the safety concerns associated with their fire performance, resulting from higher density, can call its advantages into question. As opposed to data circumscribed on compressive and tensile strength, rare are studies that have been focused on other aspects of high strength concrete, like shear strength or durability properties, in hot conditions. To conduct a thorough investigation, an experimental program embodying mechanical, durability, and microstructural aspects was performed on normal and high strength concrete in nine specific temperatures (ranging from 100 °C to 800 °C). Furthermore, a sort of relations to estimate the reduction values of mechanical properties were proposed, discussed, and compared with previous studies and standards. Although high strength concrete samples enjoyed higher capacity than normal specimens in all temperatures, their reduction rate intensified when the temperature exceeded 400 °C. The initial values for compressive, tensile, and shear strength of HSC, which were about 91.7, 5.6, and 9.5 MPa at room temperature, reduced to 28.4, 0.87, and 8.97 MPa at 800 °C, respectively. Furthermore, when temperature surpassed 400 °C, decay in high strength concrete microstructure manifested itself at durability (more than 90% growth in water absorption) and SEM images (increase in porosity) conspicuously.

Keywords: Mechanical properties, Durability, Shear strength, High temperatures, Microstructural analyze, Prediction

1. Introduction

Employing high strength concrete (HSC), instead of conventional strength one, has been growing in popularity in construction industries over recent years. Enjoying better mechanical and durability properties, HSC has wide application where a concrete with higher strength is needed, such as high rise-buildings or

*Correspondence should be addressed to: Mehrdad Abdi Moghadam, E-mail: M.abdimoghadam@edu.ikiu.ac.ir



bridges. However, in the face of high temperatures, like coal-gasification vessels, its superiority might be compromised.

Three main reasons which can contribute to the chemical and physical transformation of concrete at high temperatures are thermal incompatibility between mortar and aggregate, cracks in the cement matrix, internal stresses stemming from pore pressure, and hydration of C-S-H [1–5]. The mentioned factors can lead to microstructural decay and degrade mechanical and durability properties [1]. Adding supplementary cementitious materials into concrete mixture lead to microstructural refinement, increasing mechanical strength, but reduce permeability [6]. The impermeable microstructure of HSC at high temperatures can be counterproductive, increasing built-up pore pressure and intensifying crack propagation [3, 7]. That is why not only the HSC is prone to spalling but experiences relatively severe degradation in its mechanical properties compared with NSC. The majority of studies on HSC behavior at high temperatures have been slanted toward some typical mechanical features (such as compressive or tensile strength), overlooking other properties of concrete. In addition, few of those performed tests in the hot state [8, 9]. As per reported data on compressive strength, the residual trend can be divided typically into two phases. A fluctuated trend until 400 °C—that can be marginal [10–12] or noticeable [9, 13, 14], and a descending trend at temperatures above 400 °C. This aberrant behavior of concrete at the range of 28–400 °C can be seen in tensile behavior to a limited extent [10, 12, 15].

Concerning tests performed in the hot condition, Gyu-Yong KIM et al. [9] studied the compressive strength of HSC exposed to 700 °C. They indicated that the compressive strength variation was marginal in the range of 100 °C to 400 °C, while the main reduction branch started at a temperature above 400 °C and reached a minimum of 55% at 700 °C. Furthermore, Hugo Caetano et al. [8] studied the compressive capacity of high strength concrete during exposure, coupled with conducting image analysis on its microstructure. According to their finding, in temperature between 20 °C and 200 °C, there were no significant changes in the concrete structure, while at 200–400 °C, the dehydration of C-S-H was hastened, and between 400 °C and 700 °C, the dihydroxylation of CaCO₃ lead to calcium oxide. F.B. Varona et al. [16] examined both the compressive and tensile strength of different types of concrete. They indicated that NSC and HSC types experienced a relatively same reduction value (about 86%) in their tensile strength at temperature 825 °C, without any rising trend in the range of 28–400 °C.

As opposed to sufficient investigations on the compressive and tensile properties of HSC, increasingly less research has been done on the shear behavior of that at high temperatures. Scant information, in this case, be it in standards or publications, depicts a vague picture of the shear behavior of HSC members during high temperature exposure. However, it can be crucial when the probability of sliding failure in the cold joint- like interface between a shear wall and its foundation or web and flange of T beams [17]—coupled with detrimental effects of high temperatures on members. Generally, the shear capacity of concrete depends on some factors, including aggregate interlock, tensile strength, presence of transverse bars, the dowel action of the flexural reinforcement, the compressive strength of concrete, and characteristics of coarse aggregate [17–20]. To evaluate the shear capac-

ity of concrete, three conventional methods, namely push-off, FIP, and JSCE-G 553 are usually employed, among which, JSCE-G 553 can be more convenient and reliable when transverse reinforcements are not to be used [20]. Ahmad et al. [21] and Al-Owaisy [22] conducted push-off methods to examine the shear capacity of HSC after exposure to high temperatures. Their studies revealed that those specimens reinforced with transverse bars crossing shear plane, had a higher residual capacity and the lowest reduction rate. Also, Abdi Moghadam et al. [20] performed JSCE-G 553 to evaluate the shear strength of the plane and fibrous concrete. They proposed equations for the prediction of the shear strength of normal and steel fiber reinforced concrete exposed to high-temperature, ranging from 28 °C to 800 °C. Only does Xiao et al. [23] tried to investigate the shear transfer capacity of HSC at high temperatures by the push-off method. They examined two types of concrete with different strengths, after exposure to high temperatures, and noticed that in HSC, due to the stronger cement paste, some cracks cross over aggregate. Moreover, those specimens which enjoyed higher strength experienced severer reduction rate.

Similar to mechanical properties, the decline in the durability of concrete –whether HSC or NSC- is an indispensable part of high temperatures [4]. This decay can be mainly attributed to the irreversible chemical and physical changes during fire exposure such as water evaporation, decomposition of aggregate and hydration in cement paste; However, those materials leading to higher density can make it exacerbate, making denser structure and in turn rising pore pressure [4]. In other words, secondary cementitious materials and characteristics of aggregates (calcareous or siliceous) can play a part in the fire endurance of concrete [4, 24]. Josipa Bošnjak et al. [25] indicated that the permeability of concrete would increase nearly linearly during exposure. Furthermore, A. Mendes et al. [26] claimed that the rate of water absorption is the determining factor in controlling the extent of deterioration caused by CaO rehydration. Due to the significance of this topic and lack of standard procedure, the researchers investigating the durability properties are growing in the number over recent years. Generally, there are different methods to measure durability properties of concrete like those which are based on the water absorption test (such as capillary absorption, Sorption test, and Penetration depth) or employing electrical resistance test [1].

An evaluation of recent studies elucidated the fact that sufficient information concerning the shear and durability properties of HSC (over the course of the exposure), can be found not in the publication, nor standards. The dearth of sufficient experimental data virtually rules out the possibility of a thorough understanding of the behavior of HSC “during” high temperature exposure. This study provides not only a multifaceted investigation on the mechanical and durability properties of concrete (focusing on the less-discussed features of HSC) but also proposed equations to predict the behavior of high and normal strength concrete at high temperatures. Moreover, microstructural analysis is employed to depict an integrated assessment of concrete behavior.

2. Experimental Program

In order to satisfy the aims of the study which were the effect of the high temperatures on the mechanical and durability properties of concrete, two different kinds of concrete, one conventional with normal strength (NSC) and another high strength concrete (HSC), underwent high temperatures (100, 200, 300, 350, 400, 450, 500, 650, 800 °C). Measuring at the 28 days, the cubic strength of normal and high strength concrete was 53 and 91 MPa. Regarding concrete mixture, the Portland cement type 2 and siliceous gravel with the maximum size of 19 mm were common to both kinds of batches. However, silica fume as supplementary cementitious material (to make a more compact microstructure) together with superplasticizer (according to the ASTM C494 standard) to increase the workability, added to the high strength concrete mixture [27]. The detail of concrete mix designs is shown in Table 1.

2.1. Test Preparation

To study the mechanical properties for each mixture, 3 replica of cubic specimens (100 × 100 × 100 mm), cylindrical specimens (150 × 100 mm) and prismatic specimens (100 × 100 × 350) were assigned to examine compressive, tensile and shear strength, respectively, and the mean of those were presented. The durability test conducted on (100 × 100 × 100 mm) cubic specimens and the average of three replicate was reported in results. (Table 2). Totally, 360 specimens were casted, demolded after 24 h, and then submerged in the water bath at 24 ± 2 °C till 28 days. Before setting out heating procedure, all the specimens were stored in laboratory at temperature about 25–30 °C and 50–60% relative humidity for 14 days to avoid explosive spalling as a result of excessive moisture. An electrical-element furnace equipped with wire elements of five sides was used that was able to provide 1200 °C as maximum temperature.

2.2. Heating Procedure

An electrical-element furnace, equipped with wire elements of five sides, which were able to provide 1200 °C as the maximum operating temperature was employed to the heating regime (Fig. 1). In addition, not only were the heating rate kept in the range of 1.66–3.61 °C/min, but the specimens kept in the furnace

Table 1
Detail of Mix Designs for Normal and High Strength Concrete

Type of Concrete	Cement (kg/m ³)	Coarse aggregate (kg/m ³)	Fine aggregate (kg/m ³)	w/c	Maximum aggregate size (mm)	Silica fume (kg/m ³)	Superplasticizer (kg/m ³)
NSC	400	935	765	0.5	19	–	–
HSC	530	1030	700	0.35	19	50	4

Table 2
The Scope of Test

Target temperatures (°C)	Objects of study	Tests	Concrete types	
			NSC	HSC
			Number of specimens	
28	Mechanical properties	Compressive strength	30/cubic	30/cubic
100		Tensile strength	30/cylindrical	30 cylindrical
200		Shear strength	30/prismatic	30/prismatic
300	Durability properties	Water absorption test	30/cubic	30/cubic
350		Capillary absorption		
400		Penetration depth		
450		Electrical resistance test	30/cubic	30/cubic
500		Mass loss	30/cubic	30/cubic
650		Total	360 specimens	
800				



Figure 1. Electrical furnace and heating procedure.

for around 3–4 h, after picking the target temperatures (Fig. 2). This low compartment heating rate, together with prolonged saturation, could result in uniform temperature distribution, eliminating thermal gradients. Hence, it not merely could minimize the risk of explosive spalling but offered a thermal steady state wherein thermal gradients were minimum. Such conditions could prepare the way for making a comparison with previous studies, most of which, tended to induce uniform temperature distribution through the cross-Section [28]. Immediately after

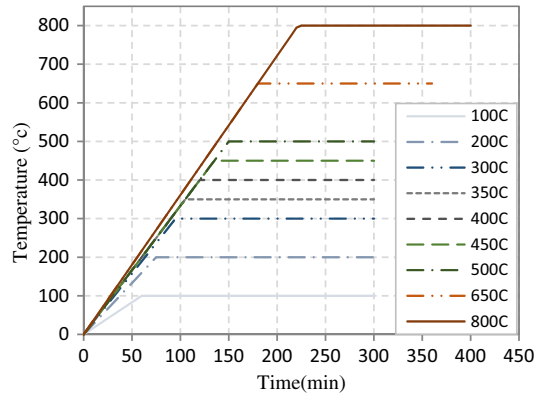


Figure 2. Time-temperature curves.

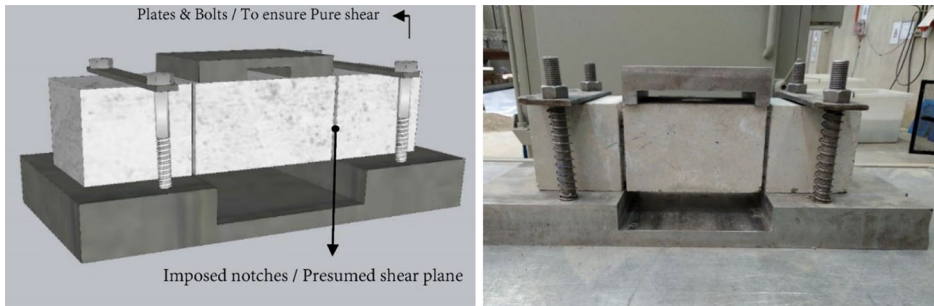


Figure 3. Direct-shear test scheme.

finishing temperature exposure, the specimens were tested, when the temperature drop was negligible.

2.3. Test Setup

2.3.1. Mechanical Tests Compression and tension tests were conducted according to the British [29] and ASTM C 496/C 496 M-04 standard [30], respectively. 100 mm cubic and 150 × 300 mm cylindrical samples were assigned to this purpose. Furthermore, to perform a direct shear test on 100 × 100 × 350 prismatic specimens, JSCE_G 553 method as per JSCE standards was adopted [31]. In this method, to dictate a shear plane for assets pure shear, notches of 5 mm width and 10 mm depth were exerted on the concrete surface, and bolts clamped specimens on the base. A loading block was responsible for applying the shear load on the specimen placed on two rigid blocks with a central free span equal to 155 mm. The test scheme is shown in Fig. 3.

2.3.2. Durability Tests Two different kinds of durability tests- namely water absorption and electrical resistance-were performed to evaluate the durability properties of 100 mm cubic specimens exposed to high temperatures. As for water absorption tests, firstly, lateral surfaces of specimens were sealed with epoxy resin, and then samples were immersed in water to a certain depth (30 mm), where water was allowed to penetrate the concrete (Fig. 4a). Furthermore, they were weighted before immersing and at the intervals of 3, 6, 24, 48, 72 h after that. Afterward, capillary absorption and penetration tests were calculated.

To determine Capillary absorption, the following formula is used [4].

$$Q = A \times K\sqrt{t}$$

Q is the amount water absorbed (cm^3), A is the cross-sectional area of the specimens that is contact with water (cm^2), T is time (s), and K is capillary absorption coefficient ($\text{cm}/\text{s}^{1/2}$). Figure 16 shows the variation of K in target temperatures.

To measure electrical resistance, specimens were submerged into a water tank for 24 h to uniformly saturate, and then the electrical resistance was performed on specimens in two perpendicular directions after de-molding (Fig. 4b). The test measures the conductivity, normalized to the cross-sectional area, of electricity through a concrete sample.

The following formula can be used to calculate the specific electrical resistance.

$$r = \frac{R \times A}{L}$$

- R (Ω) is the electrical resistance
- A (m^2) is the concrete surface area
- L (m) is the sample length
- r ($\Omega\cdot\text{m}$) is the specific electrical resistance

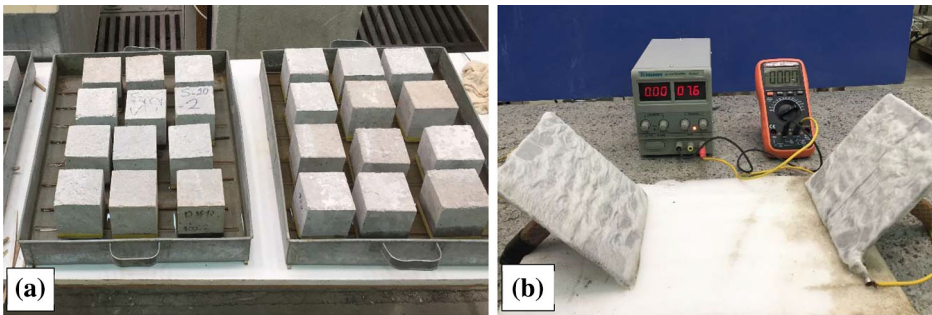


Figure 4. Preparation of specimens for durability tests: (a) Based on water absorption (b) Based on electrical resistance.

2.3.3. Microstructural Analyze Thermal gravity analysis (TGA) was conducted to a better understanding of chemical reactions of concrete caused by temperatures. To this purpose, specimens derived from core of concrete samples were ground to pass through a 70 m sieve, and then they studied by Pyris Diamond TG/DTA thermal analyzer at a heating rate of 10 C/min under nitrogen atmosphere. Concerning the scanning electronic microscopy test (SEM), specimens-at the approximate size of $0.5 \times 1 \times 1$ -were extracted from the core of specimens, tested by Philips XL-30 scanning electron microscope. To prevent the repelling of electrons that were emitted by the device, the surfaces of the specimens were coated with a gold alloy film.

3. Results

3.1. Mechanical Properties

3.1.1. Compression In this study, cubic specimens, after experiencing target temperatures and before cooling done, were tested according to the British standards [29]. The primary results are shown in Table 3.

Figure 5 provides a comparison between the compressive strength of NSC and HSC at different temperatures. As could be observed, the initial compressive strength of HSC at room temperature was about 92 MPa (1.72 times more than the strength of NSC at the same temperature). By rising temperature to 100 °C, both types of concrete experienced an abrupt reduction, reaching around 81 and 38 MPa, respectively. Since at this temperature chemical changes are not significant, this reduction can be attributed to the evaporation of free water in capillary pores, and in turn, increasing the internal pressure [14]. When the temperature increased from 200 °C to 400 °C, the strength again started to rise (both for HSC and NSC) and exceeded the initial strength of HSC at room temperature. This behavior grows out of rehydration and hardening in cement gel [32]. The strength

Table 3
Compressive Strength of NSC ad HSC at High Temperatures

Concrete T(°C)	HSC			NSC		
	AVG	St.Dev	C.o.V (%)	AVG	St.Dev	C.o.V (%)
28	91.70	3.01	3.28	53.19	2.70	5.08
100	81.80	7.23	8.84	38.11	1.14	2.98
200	90.73	0.75	0.83	46.19	2.25	4.87
300	100.10	1.30	1.30	50.16	0.43	0.85
350	99.70	4.85	4.87	52.40	2.25	4.29
400	92.10	1.93	2.10	49.32	1.74	3.54
450	89.17	1.93	2.16	43.66	2.59	5.93
500	81.47	5.86	7.19	39.38	3.43	8.70
650	44.47	1.50	3.38	23.80	2.11	8.86
800	28.47	2.67	9.38	13.88	0.59	4.25

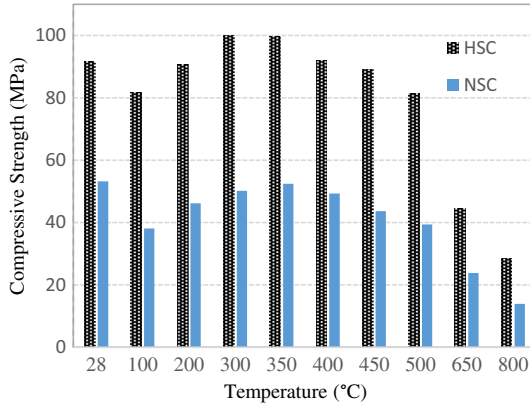


Figure 5. Compressive strength of HSC and NSC by temperatures.

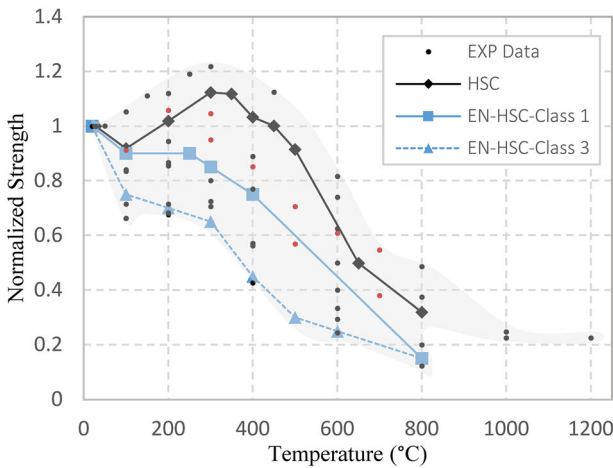


Figure 6. Normalized reported data on compressive strength of HSC.

of specimens (which were about 92 and 50 MPa for HSC and NSC at 400 °C) reduced by rising temperature, reaching a minimum at around 28 and 13 MPa at 800 °C, consecutively. What makes differences between NSC and HSC is the dense structure of HSC that intensifies the reduction rate. In other words, from 400 °C to 800 °C, the compressive strength of HSC reduced at a relatively higher rate compared with NSC. Moreover, the final capacity of HSC at 800 °C was about 30% of initial strength (28.48 MPa), while the figure for NSC was about 26% (13.88 MPa) (Fig. 5).

Figure 6 gathered data of authentic studies over recent years along with compressive test results of the current study and EN prediction. The shaded area, which embodies dots, illustrates a spectrum of variation of results reported by

previous researchers (the black dots represent compressive strength after cooling down, and red ones are related to testing in hot conditions) [8–16, 33, 34]. As can be seen, the maximum deviation occurs at 400 °C, which embodies ranging between 0.4% to 1.2%. The reduced compressive strength of HSC posited by Eurocode was depicted for two different classes of high strength concrete (class one: C55/67 and class three: C90/105), as well [35]. Figure 6 clearly illustrates a deviation between reported data on HSC, the reason of which can be due to the different test conditions (duration of exposure, heating rate, and casting) or may be attributed to the unpredictable behavior of that in high temperatures (as a result of the built-up pore pressure, and in turn spalling) [7].

According to the reduction values of HSC and NSC, the reduced compressive strength can be defined as:

$$f_{c,\theta} = \emptyset \times (f_{c,i})$$

In which $f_{c,\theta}$ is the compressive strength of concrete at the target temperature, θ is experienced temperature, $f_{c,i}$ is the initial strength, and \emptyset is the reduction coefficient according to Table 4:

3.1.2. Tension There are different methods to evaluate the tensile strength of concrete, such as the direct tension test, pull-off, and splitting tensile strength. The two first have been mostly used for HSC and UHPC, especially for determining the bond strength between interfaces, estimating lower capacity than splitting test. On the other hand, the splitting tensile test has been frequently employed by different researchers for different types of concretes. The advantage of the latter is the ease of use, especially at elevated temperature, and an extensive data set for the comparison. Before initiating the heat process, the correlation between the compressive and tensile strength for different concrete classes was examined, compared, and presented in Fig. 7 and Table 5. As can be seen, the correlation between compressive and tensile strength in this study had a good agreement with the formula proposed by other researchers and standards. However, a few of those had a steeper slope than others.

When spalling is concerned, the role of tensile can be of paramount importance [10]. In this study, to examine reduced tensile strength of concrete stemmed from high temperatures, the specimens fabricated with normal and high strength con-

Table 4
Reduction Values for HSC and NSC by Temperatures

T (°C)	T < 400		T ≥ 400	
	\emptyset	R ²	\emptyset	R ²
NSC	$(-6 \times 10^{-8})T^3 + (4 \times 10^{-5})T^2 - 0.0073T + 1.1585$	0.87	$-0.0017T + 1.5824$	0.99
HSC	$(-4 \times 10^{-8})T^3 + (2 \times 10^{-5})T^2 - 0.0036T + 1.0818$	0.99	$-0.002T + 1.8453$	0.97

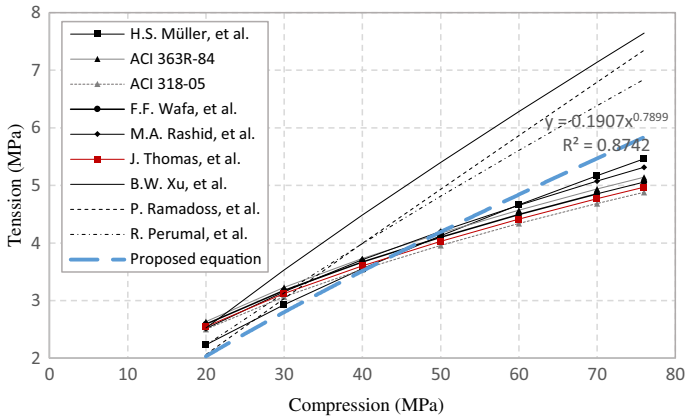


Figure 7. Correlation between tensile strength (f_t) and compressive strength (f_c).

Table 5 Proposed Equations for the Tensile Strength of Plain Concrete

Reference	Equation (MPa)	Reference	Equation (MPa)
H.S. Müller et al. [36]	$f_t = 0.3 \times (f_c)^{0.67}$	J. Thomas et al. [37]	$f_t = 0.57 \times (f_c)^{0.5}$
ACI 363R-84 [38]	$f_t = 0.59 \times (f_c)^{0.5}$	B.W. Xu et al. [39]	$f_t = 0.21 \times (f_c)^{0.83}$
ACI 318-05 [40]	$f_t = 0.56 \times (f_c)^{0.5}$	P. Ramadoss et al. [41]	$f_t = 0.12 \times (f_c)^{0.95}$
F.F. Wafa et al. [42]	$f_t = 0.58 \times (f_c)^{0.5}$	R. Perumal et al. [43]	$f_t = 0.18 \times (f_c)^{0.84}$
M.A. Rashid et al. [44]	$f_t = 0.47 \times (f_c)^{0.56}$	Proposed equation	$f_t = 0.19 \times (f_c)^{0.78}$

Table 6 Tensile Strength of NSC ad HSC at High Temperatures

Concrete T (°C)	HSC			NSC		
	AVG	St.Dev	C.o.V (%)	AVG	St.Dev	C.o.V (%)
28	5.66	0.73	12.82	3.03	0.26	8.67
100	4.84	0.69	14.27	2.11	0.18	8.39
200	4.48	0.29	6.52	0.92	0.05	5.80
300	3.82	0.30	7.73	1.85	0.24	12.91
350	3.20	0.34	10.66	2.16	0.12	5.74
400	2.94	0.22	7.36	2.52	0.24	9.46
450	2.99	0.44	14.74	1.55	0.14	9.32
500	2.51	0.09	3.62	1.51	0.34	22.38
650	1.46	0.07	4.67	0.75	0.06	8.01
800	0.87	0.02	2.30	0.69	0.03	4.00

crete- after experiencing target temperature- were immediately tested by tensile testing recommended by ASTM C 496 [30]. Table 6 and Fig. 8 provide information about the average tensile strength values of NSC and HSC in the target temperatures. Tensile strength of concrete members is significantly lower than compressive ones; however, the factors that affect tensile strength are almost the same for both.

What can be noticed at first glance is about an anomaly in the behavior of NSC specimens at the range of 28–400 °C. In other words, while high strength concrete experienced a steady reduction rate, normal strength ones represented an up and down figure. When the temperature rose from 28 °C to 200 °C, both types of concrete experienced a reduction; however, it was far more intensive in NSC. The initial tensile strength of NSC samples (which was 3.03 MPa) with 70% reduction, reached a mere 0.92 MPa at 200 °C, while HSC samples experienced about 20% reductions in the temperature. The reasons for this aberrant behavior can be summarized into two facts: (1) Since in this temperature, the mortar has acceptable tensile strength, this decline can be attributed to the simultaneous effect of applied load and the outward pressure of water stream [1]; (2) evaporation of free water that can exacerbate the internal pressure. Since the amount of free water in NSC was higher than HSC, this reduction was completely conspicuous for those. It should be pointed out that the failure of specimens at a temperature between 100 °C and 200 °C was accompanied by load noise and intensive releasing water stream.

At temperature range of 200–400 °C, although HSC continued to its previous trend, and reduced to about 50%, NSC samples regained 80% of their initial strength. As will be expounded in the following section, the hydration of un-hydrated cement and enhancement in the inner force of cement gel can be responsible for this. At temperature above 400 °C, the descending trend was predominant for both types of concrete. NSC samples had a rapid reduction rate between 400 °C to 450 °C, and then, attained the same figure with HSC specimens until 800 °C. The final residual tensile value for NSC and HSC, at 800 °C, was about

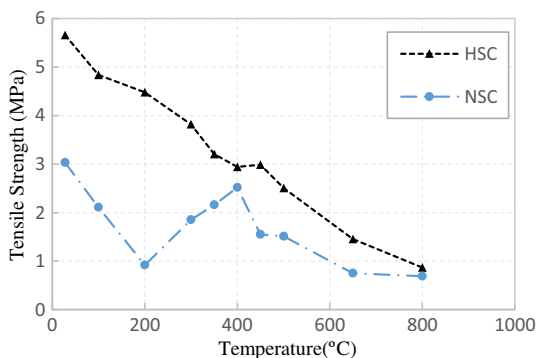


Figure 8. Tensile strength of NSC and HSC by temperatures.

0.69 and 0.87 MPa, respectively. Although the reduction rate was relatively severe for HSC, it had greater tensile values in all temperatures than NSC.

The failure pattern of HSC samples consisted of longitudinal and lateral cracks on the specimen's surface while it turned into longitudinal cracks at temperatures above 400 °C (Fig. 9).

According to the Fig. 9 reduced tensile strength can be defined as a function of initial strength and temperature as below:

$$f_t = 0.19 \times (f_c)^{0.78} \quad (1)$$

And

$$f_{t,\theta} = \lambda \times (f_{c,i}) \quad (2)$$

In which $f_{t,\theta}$ is the tensile capacity in target temperatures, $f_{c,i}$ is the primary tensile strength, and λ is the reduction coefficient. From a combination of (1) and (2):

$$f_{t,\theta} = \lambda \times 0.19 \times (f_c)^{0.78} \quad (3)$$

The reduction values (λ) according to the type of the concrete (normal or high strength) can be attained form following Table 7, in which T is the target temperature in centigrade.

There are some experimental works wherein the tensile strength of the HSC has been examined under high temperatures, most of which were after cooling down. Moreover, the number of relations which aim to estimate the reduced tensile strength of HSC is not considerable, Compared with NSC. Equation was compared with the latest authentic data on the HSC at high temperatures to ensure reliability (Table 8 and Fig. 10).

According to Table 8 and Fig. 10, although the accuracy of the proposed formula to estimate the reduced tensile strength is acceptable in some cases [10, 13,

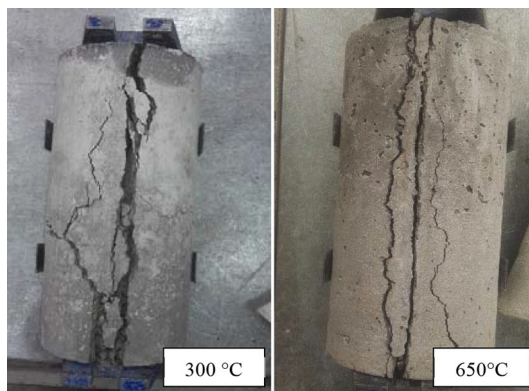


Figure 9. Failure patterns of HSC specimens.

Table 7
Reduction Values for HSC and NSC by Temperatures

T (°C)		λ	R ²
NSC	T ≤ 400	$1.514 \times 10^{-5}T^2 - 6.76 \times 10^{-3}T + 1.18$	0.88
	T > 400	$3 \times 10^{-6}T^2 - 4.62 \times 10^{-3}T + 2.02$	0.95
HSC	28 < T ≤ 800	$-1.1 \times 10^{-3}T + 0.9903$	0.98

Table 8
Validation of Experimental and Calculated Tensile Strength

Reference	Test program	f_c (MPa)	Temperature (°C)	Experimental Tensile strength (MPa)	Calculated Tensile strength (MPa)	Ratio of Ex/Ca
Bing Chen et al. [15]	Cooled up to 800 °C	Cubic 82 MPa	28	8.00	7.67	1.04
			200	8.00	6.16	1.29
			400	3.50	4.40	0.79
			600	1.70	2.64	0.64
			800	0.60	0.88	0.67
Reza Abaician et al. [13]	Cooled up to 300 °C	Cubic 69 MPa	20	12.00	11.61	1.03
			100	11.00	10.56	1.04
			200	10.00	9.24	1.08
			300	8.50	7.92	1.07
F.B. Varona et al. [16]	Cooled up to 850 °C	Cubic 89 MPa	20	3.90	3.77	1.03
			450	2.60	1.93	1.34
			650	1.00	1.07	0.93
			825	0.77	0.32	2.38
Wasim Khaliq et al. [12]	Cooled up to 800 °C	Cylindrical 70 MPa	28	5.10	4.89	1.04
			100	3.50	4.48	0.77
			200	3.60	3.92	0.91
			400	2.50	2.80	0.89
			600	1.80	1.68	1.06
Ali Behnood et al. [10]	Cooled up to 600 °C	Cylindrical 75 MPa	28	5.50	5.27	1.04
			100	4.60	4.84	0.95
			200	4.70	4.23	1.10
			300	4.30	3.02	1.42
			600	1.40	1.81	0.77

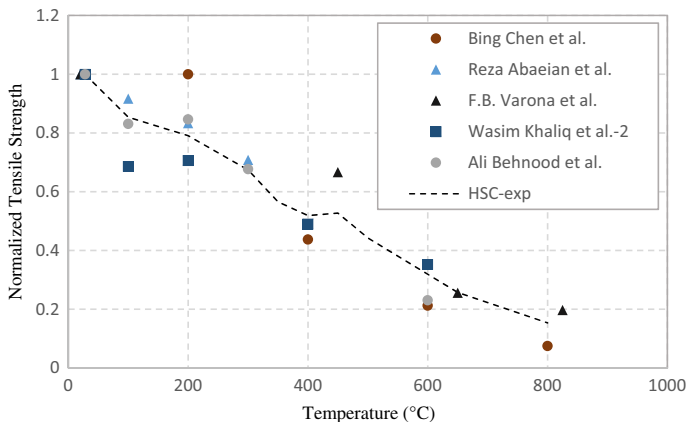


Figure 10. Normalized experimental data on tensile strength of HSC at high temperatures.

16], it is not able to predict accurately in other cases [12, 15], especially at the range of 28–400 °C. This difference between results can be attributed to the different test conditions, fire scenarios, and spalling or secondary cementitious materials used in cement paste. Surprisingly, rare are experimental data that have investigated the tensile capacity of HSC in hot conditions. Thus, this study may give a better insight into this case.

3.1.3. Shear Concerning reduced mechanical strength (tensile, compression, and flexural) caused by high temperatures, Shear capacity of concrete has received less attention than others. The shear capacity is due to a large extent to the compressive strength of concrete, friction between cracked surface and, aggregate interlocking mechanism [17, 45]. Among different methods for the shear test, in this study JSCE_G 553 was chosen. As opposed to the Hoffbeck style push-off and FIP, this method is more convenient and less complicated, especially when the experiment is to be done at elevated temperatures. Moreover, it is able to provide a pure shear stress field.

To obtain a correlation between the compressive and shear strength of concrete at room temperature, shear and compressive tests were conducted on specimens with different concrete grades (ranging from C25/30 to C70/85). In addition, a number of equations derived from previous studies were compared with the results that can be observed in Fig. 11 and Table 9. According to the regression analysis provided in Fig. 12, the gradient of the proposed equations was around 0.05, with a moderate increasing rate. However, in some cases, like the equation suggested by Boulekbache et al. [18], it raised to about 2.4. This discrepancy can be attributed to the type and size of coarse aggregate which have noticeable impact on shear behavior of concrete.

Table 2 and Fig. 12 represent the normalized and experimental values of the test, and Fig. 13 shows the cross-section of specimens after the shear test. At first

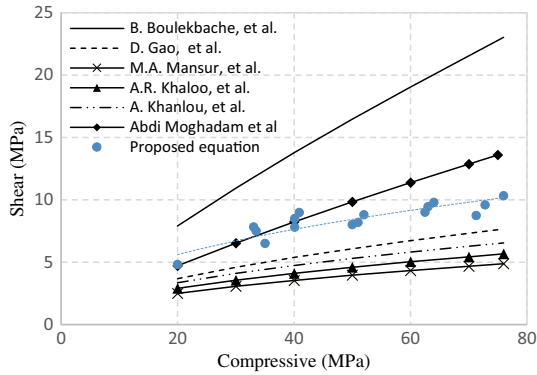


Figure 11. Correlation between shear (τ) and compressive strength (f_c).

**Table 9
The Proposed Equation for Shear Strength of NSC**

References	Equation (MPa)
B. Boulekbache et al. [18]	$\tau = 0.72 \times (f_c)^{0.8}$
D. Gao et al. [19]	$\tau = 0.8 \times (f_c)^{0.55}$
M.A. Mansur et al. [46]	$\tau = 0.56 \times (f_c)^{0.5}$
A.R. Khaloo et al. [47]	$\tau = 0.65 \times (f_c)^{0.5}$
A. Khanlou et al. [48]	$\tau = 0.75 \times (f_c)^{0.5}$
Abdi Moghadam et al. [20]	$\tau = 0.43 \times (f_c)^{0.8}$
Proposed equation	$\tau = 1.46 \times (f_c)^{0.45}$

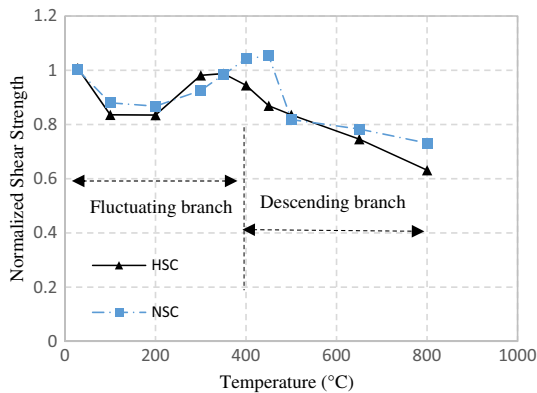


Figure 12. Normalized residual shear strength of NSC and HSC at high temperatures.



Figure 13. Direct shear tests setup- shear plane.

glance, likewise the compressive strength, two main phases can be noticed: first, a fluctuated trend at the temperature between 28 °C and 400 °C, and second, a descending trend at a temperature above 400 °C. As for NSC, the initial shear strength at room temperature was about 8.44 MPa, followed by a drop at 100 °C (Fig. 13). This sudden reduction resulting from the evaporation of free water is nearly 12%. When the temperature rose from 100 °C to 450 °C, the strength reached to 8.88 MPa (nearly 5% more than initial strength). This ascending branch, which occurred both in normal and high strength samples, can be related to the restrengthening of the cement matrix. XRD results in previous studies confirm this [32]. As mentioned earlier, weakness in the interlocking mechanism of concrete (as a result of thermally-induced stress across the interface transition zone between the aggregate and the cement paste) can bring about detrimental effects on shear strength. When the temperature rose from 200 °C to 400 °C, rehydration of cement paste caused reinforcing the cement matrix again, and in turn, ameliorate the bond interaction between components. Because of that, in both concrete types, an improvement in shear strength was observed in the mentioned range. Interestingly, this figure was also observed earlier in compressive strength, which has a significant impact on shear strength [45]. Through the descending phase, increased strength of concrete at 450 °C reduced by 20% at 500 °C, and then, reaching to 6.16 MPa at 800 °C. Regarding HSC, the shear capacity, which was about 9.5 MPa in 28 °C, was accompanied by 20% reduction at 100 °C and 200 °C, soaring to the primary strength (just below 9.5) at 300 °C and 350 °C. Then, with a steady reduction rate, it reached a minimum of 5.97 MPa at 800 °C. In the aggregate, the final strength for NSC was 73%, while the figure for HSC was around 62% (Table 10). Although the HSC, due to the stronger bond between aggregate and cement paste, had a slightly better performance than NSC, their reduction rate was relatively higher compared with normal strength samples.

Table 10
Shear Strength of NSC Ad HSC at High Temperatures

Concrete T(°C)	HSC			NSC		
	AVG	St.Dev	C.o.V (%)	AVG	St.Dev	C.o.V (%)
28	9.53	0.80	8.41	8.44	0.42	4.98
100	7.90	0.50	6.36	7.42	0.6	8.13
200	7.89	0.38	4.77	7.31	0.65	8.87
300	9.28	0.39	4.17	7.80	0.46	5.93
350	9.34	0.37	4.00	8.29	0.77	9.33
400	8.93	0.17	1.86	8.78	0.17	1.97
450	8.22	1.18	14.38	8.88	0.63	7.13
500	7.90	0.09	1.08	6.89	0.75	10.81
650	7.05	0.82	11.58	6.60	0.4	6
800	5.97	0.87	14.53	6.16	0.52	8.5

This behavior can be attributed to developing cracks on microstructure to a greater extent than NSC [45].

The shear strength of concrete at high temperatures, can be defined as a function of compressive strength together with a reduction coefficient (α) based on the experimental data. Thus:

The correlation between compressive strength at room temperature can be achieved by:

$$\tau_i = 1.46 \times (f_c)^{0.45} \quad (4)$$

f_c = cylindrical compressive strength. The shear strength of concrete at high temperatures can be defined:

$$\tau_\theta = \alpha \tau_i \quad (5)$$

In which τ_θ is the shear transfer capacity of concrete at each temperature, τ_i is the primary shear strength, and θ is the reduction coefficient. From combination of (4) and (5):

$$\tau_\theta = \alpha \times 1.46 \times (f_c)^{0.45} \quad (6)$$

The reduction values (α) according to the type of the concrete (normal or high strength) can be attained form Table 11:

Figure 14 provides a comparison between the experimental results of the current study with the calculated values form Eq. 6. As can be seen, the posited formula has relatively good agreement with the experimental results. However, there is a subtle disparity between real and assessed data, the roots of which can be

Table 11
Reduction Values for HSC and NSC by Temperatures

T (°C)	T < 400		T ≥ 400		R ²
	α	R ²	α	R ²	
NSC	$(5.11 \times 10^{-6})T^2 - 0.0019T + 1.04$	0.95	$(2.76 \times 10^{-6})T^2 - 0.0041T + 2.268$	0.85	
HSC	$(-4.04 \times 10^{-8})T^3 + (2.93 \times 10^{-5})T^2 - 0.00576T + 1.1505$	0.98	$(-8 \times 10^{-4})T + 1.238$	0.98	

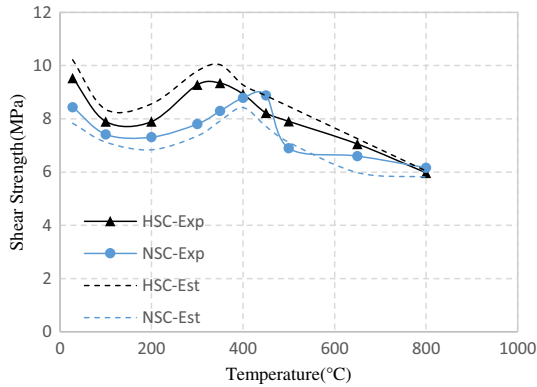


Figure 14. Comparison between experimental and estimated values by the proposed equation.

summarized into an estimated trend between compressive and shear strength in Eq. 4 and converting cubic strength to cylindrical.

Over recent years, different researchers try to investigate the shear strength of concrete, most of whom aimed at studying normal strength concrete after “cooling down” [17, 21, 45]. While a group utilized reinforcements crossing the shear plane (in order to provide a clamping force between sliding faces), others ignored it in favor of studying shear capacity of concrete. Among the recent studies, only Xiao et al. [23] investigated the shear behavior of high strength concrete members exposed to high temperatures. Using of two types of concrete with different strength, they conducted Push-off methods (reinforced with transverse on the interface) to examine residual shear transfer strength of concrete after exposing to high temperatures. Drawing a comparison between experimental data derived from Xiao’s work with the values calculated by Eq. 6 discloses a difference between real and predicted values at ranging of 1% to 32%. This may be attributed to different test conditions, such as performing the push-off method, using transverse bars, or testing after cooling down instead of the hot state (Table 12).

On the other hand, concerning standards, Eurocode proposed a simplified approach, in which the degraded shear strength of concrete members can be projected by using reduced strength of materials that is suggested by EN 1992-1-2 (tabulated data about reduction value of compressive strength for NSC and HSC), and methods to calculate shear strength which is given in EN 1992-1-1 [35, 49]. As can be seen from Table 4, the estimated values by Eurocode for this study have a significant deviation with values calculated by Eq. 6. Moreover, this gap widens by increasing temperature, where at 800 °C it reached about 91%.

3.2. Durability Properties

As far as degraded properties of concrete are concerned, durability properties are due to an extent to the microstructural deterioration. High temperatures induce detrimental effects to microstructural integrity, degrading the durability properties.

Table 12
Comparison Between Reduction Values in Shear Transfer Capacity of Previous Studies, Eurocode, and Current Study for HSC

Reference	Xiao [23]				Eurocodes [35]				
	Push-off method/after cooling down				Simplified approach				
Method									
Concrete class	C50/60				C70/85				
MPa									
°C									
	Experimental data	Calculated data (Eq. 3)	$ \Delta (\%)$	Experimental data	Calculated data (Eq. 3)	$ \Delta (\%)$	Calculated data/EN	Calculated data (Eq. 3)	$ \Delta (\%)$
28	9.93	8.71	12.2	11.9	10.30	13.44	4.76	9.64	50.62
100	–	–	–	–	–	–	3.57	7.93	55
200	9.28	7.3	20.3	12.87	8.63	32.9	–	–	–
400	8.04	8.19	1.83	9.22	9.69	4.85	3.57	8.86	59.7
800	4.67	5.15	9.32	5.22	6.09	14.28	0.71	8	91.12

This degradation in durability properties can also manifest itself in the mechanical properties of concrete. In other words, durability properties are an indicator of microstructural deterioration that can contribute to predicting mechanical properties. This fact is mostly highlighted in structures wherein high temperatures are an indispensable part, like industrial chimneys. As opposed to the mechanical properties of concrete at high temperatures, durability properties have failed to attract attention. Generally, the durability of concrete can be determined using various techniques, among which water absorption tests and electrical resistance have been deployed in this study.

3.2.1. Capillary Absorption Tests The capillary absorption test is a way in which the capacity of concrete in absorbing water will be measured to determine the extent of voids, cracks, and porosity. The test procedure has been also discussed earlier in experimental program section (Figs. 4a, 15). As can be seen from Fig. 16, the damaged structure of concrete tends to absorb more water at earlier hours in both types of concrete. However, by rising temperature, as opposed to NSC, deviation in capillary absorption coefficient (K) between the intervals (3, 6, 24, 48, and 72 h) became more and more tangible in HSC samples. In other words, the amount of water absorbed by HSC samples during first intervals (3 h) was 4.75 times higher than the last interval (72 h), while this figure for NSC was 2.25 at 800 °C. In addition, the coefficient of K in HSC was more sensitive to

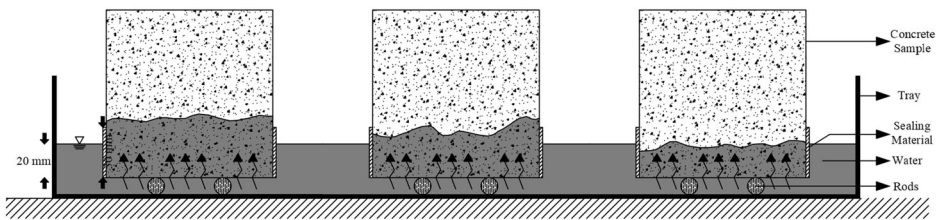


Figure 15. Schematic illustration of water absorption test setup [1].

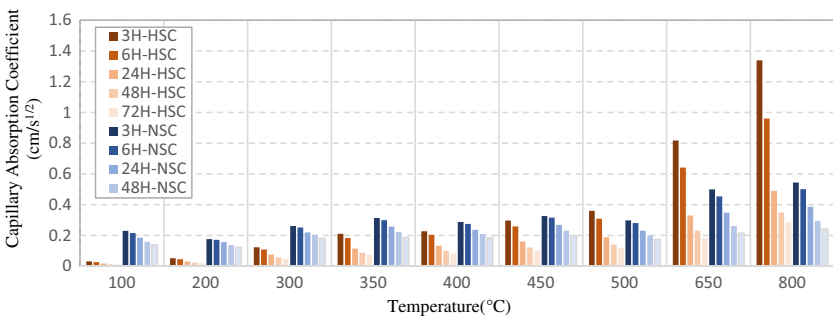


Figure 16. Values of the capillary absorption coefficient for NSC and HSC at high temperatures.

temperature variation. Whereas this figure for NSC had a range of 0.2 to 0.6 $\text{cm/s}^{1/2}$, HSC had a range of 0 to about 1.4 $\text{cm/s}^{1/2}$.

450 °C was a turning point for HSC, in which the water absorption of HSC samples overtook of NSC ones. Based on the average, the values of k , which were about 0 and 0.2 $\text{cm/s}^{1/2}$ for HSC and NSC at 100 °C, rose to 0.18 and 0.26 $\text{cm/s}^{1/2}$ at 450 °C. Above this temperature, although the NSC continued to its steadily increasing rate and reached 0.39 $\text{cm/s}^{1/2}$, the HSC soared at an increasingly rapid rate, reaching maximum at 0.68 $\text{cm/s}^{1/2}$ at 800 °C. This increase is clearly noticeable when the first hours of the test are to be concerned. It goes without saying, the microstructure of NSC consists of more voids than HSC. Because of that, the water absorption was higher in normal strength samples at a low temperature, when the concrete degradation is not significant. By the increase in temperature, the HSC-which enjoy a denser microstructure- became more vulnerable to crack propagation, having more tendency to absorb water. The figure was also aggravated by higher temperatures. Hence, those supplementary cementitious materials, such as silica fume that can refine the microstructure (together with greater cement content, and denser aggregates), alleviating the mechanical strength of concrete at room temperature but can contribute to the deterioration in concrete durability at high temperatures.

3.2.2. Penetration Depth The penetration depth is another factor that can determine the extent of microstructural decay of concrete. Having a similar test setup with previous method, the penetration depth test can be achieved by measuring the average height of the water column in the cross-section of specimens during given intervals. Figure 17 represents the average depth of water ingress into the concrete structure for NSC and HSC after 72 h immersion.

Containing more voids in their structure, the normal strength specimens experienced higher penetration depth. This amount for NSC was about 60 mm at 100 °C, followed by a 40% growth, reached to 100 mm at 400 °C. After a decline (about 20%) at temperature 400–500 °C, it again reached to 100 mm at tempera-

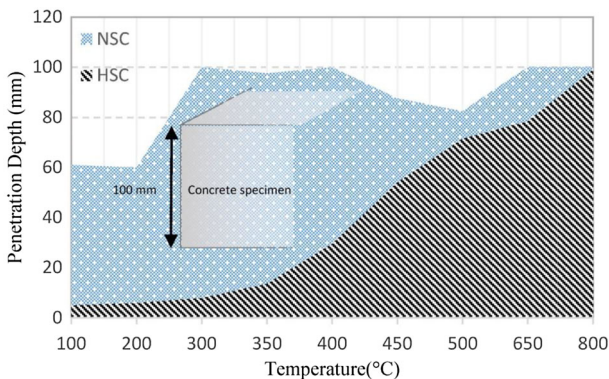


Figure 17. Variation of water penetration depth in NSC and HSC at temperatures.

tures above 650 °C. On the other hand, being more susceptible to water ingress due to the aforementioned reasons, HSC had a dramatically increasing rate when the temperature exceeded 400 °C. When the temperature increased from 100 to 350 °C, penetration depth rose to 20 mm, while at 800 °C, it reached the maximum at 100 mm (water penetrated the whole cross-section).

3.2.3. Electrical Resistance The electrical resistance test is another method that can be employed for evaluation durability of concrete. This test is representative of how difficult it is for an electrical current to get from one end of the sample to another. In other words, it measures the electrical resistivity of the concrete pore solution. It can be used to examine chloride ion diffusivity, concrete resistivity in a hostile environment, and corrosion of steel bars, as well [50, 51].

As the temperature rose, so did the water absorption; specific electrical resistance did not follow the trend and went decreased. In other words, there is inverse nexus between those. As opposed to the NSC, which had a moderately decreasing rate, and reduced from around 70 $\Omega\cdot\text{m}$ at 100 °C to less than 25 $\Omega\cdot\text{m}$ at 800 °C, the electrical resistance of HSC rapidly fell by temperature growth. However, the sharp division between those become blurred by rising temperatures (Fig. 18). The initial electrical resistance of HSC at 100 °C was 320 $\Omega\cdot\text{m}$ —4 times more than the electrical resistance of NSC at the very temperature. However, as a result of increasing temperature, it precipitously declined to less than 150 $\Omega\cdot\text{m}$ at 300 °C. What makes the difference between the water absorption test and electrical resistance is the starting time of the main variation trend in HSC samples. In other words, the water absorption increased suddenly form 450 °C, which can be attributed to the crack propagation and creation voids in microstructure, while this figure for electrical resistance occurred between 200 °C and 300 °C. Since in these temperatures, the mechanical degradation of structure cannot be acute, this increase may result from severe chemical changes in the cement matrix of HSC.

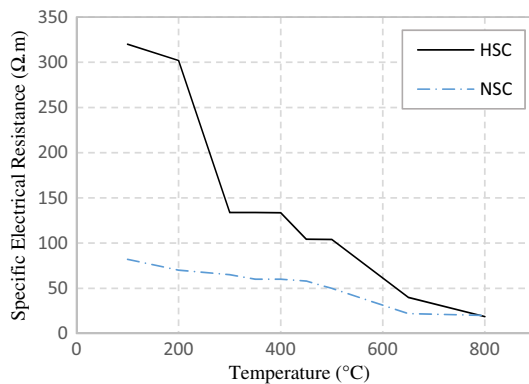


Figure 18. Variation of specific electrical resistance in NSC and HSC at high temperatures.

At temperature above 400 °C, the values of “r” reduced for HSC but at a moderate rate until 800 °C that ended in 19 Ω.m, not unlike NSC (Fig. 18).

According to Fig. 19, in one taxonomy the electrical resistance of HSC can be divided into three different stages: first at the range of 100 to 300 °C, wherein the proportion of “r” were about 20% and 60% for NSC and HSC, respectively. Second, at the range of 300–500 °C that the figure remained constant for NSC at 20% and decreased for HSC to 10%. And the final stage, in which the percentage of “r” decreased to 24% and 5% for NSC and HSC when the temperature rose from 500 to 800 °C. Moreover, it is worth mentioning that the total reduced specific electrical resistance for NSC and HSC were 76 and 95%, consecutively.

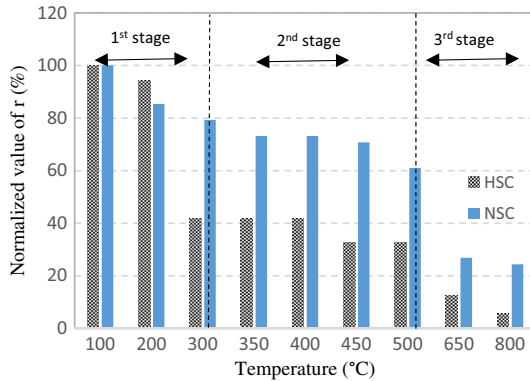


Figure 19. Normalized values of specific electrical resistance of NSC and HSC by temperatures.

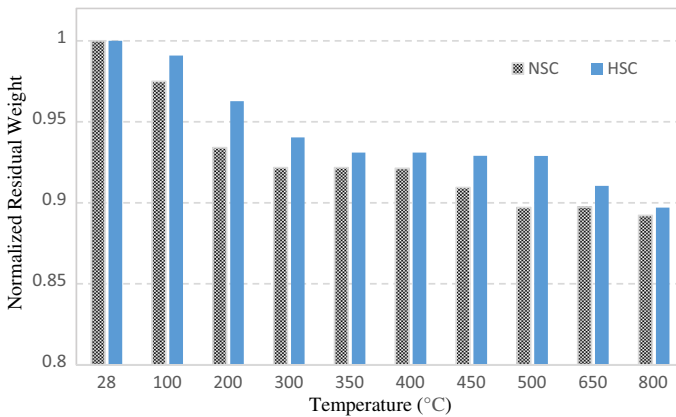


Figure 20. Normalized mass loss of NSC and HSC specimens at high temperatures.

3.2.4. *Mass Loss Reduction* in mass or density of concrete due to the loss of moisture is an inevitable by-product of high temperatures. To find the effect of that, the cubic specimens were weighted before and after exposure to high temperatures. Figure 20 indicates the variation of residual mass at different temperatures. In general speaking, the strength of concrete did not have an obvious impact on weight loss, and both NSC and HSC specimens follow a relatively similar trend. However, more moisture of NSC could give rise to more reduction of mass, compared with HSC.

3.3. Micro Structural Analysis

3.3.1. *Thermal Gravity Analysis (TGA)* Thermal gravity analysis was performed to investigate the impacts of high temperatures on the hydration process of concrete. The previous study done by Abdi Moghadam et al. [32] on normal mortar demonstrated that those specimens which had enjoyed better mechanical properties experienced a lower weight loss in the TGA test. The results of Fig. 12 provided proof of their funding on high strength concrete. According to the results, the weight loss of NSC and HSC specimens at 100 °C was about 19% and 7.5%. In addition, the proportion of that for HSC samples was always higher than NSC ones in all temperatures (Fig. 21). A comparison between the results of the TGA test on heated and non-heated specimens illuminated that at temperatures below 200 °C—where evaporation of free water is a contributing factor to weight loss—the disparity between results is conspicuous. Furthermore, according to the plots, the major weight loss occurred when the temperature in TGA tests exceeded the experienced temperature in samples. In other words, NSC and HSC samples at 400 °C showed just 5% weight loss, while in the higher temperatures this figure went noticeably increased.

When the temperature increased to 400 °C, another phase in weight loss- that was mainly due to the C–S–H gel decomposition- occurred in the specimens. In addition, another reduction phase was observed at 650 °C, where decomposition

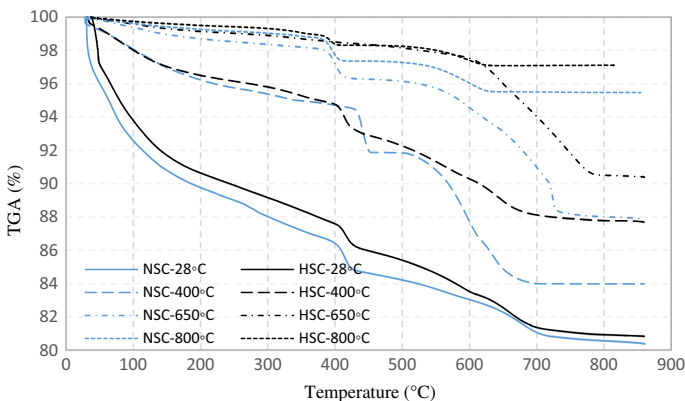


Figure 21. TGA test results for NSC and HSC samples at 28, 200, 400, 650, and 800 °C.

of CaCO_3 into CaO and CO_2 , and evaporation of CO_2 could contribute to this behavior. As a result of temperature growth, the proportion of weight loss went decrease, until the slope of the curve reached an even variation (zero-slope stage). The zero-slope stage signifies the fact that there are no other components to hydrate. In contrast, hydration for reference specimens was continued until 850°C . Another point concerning the zero-slope stage is about the start time. The temperature corresponding to the zero-slope stage is about the start time. Generally, was higher than NSC. In other words, they had more cement-based products to hydration, even at higher temperatures. Moreover, the final descending branch-before starting zero slope stage-was started from the lower temperature, for those specimens that expe-

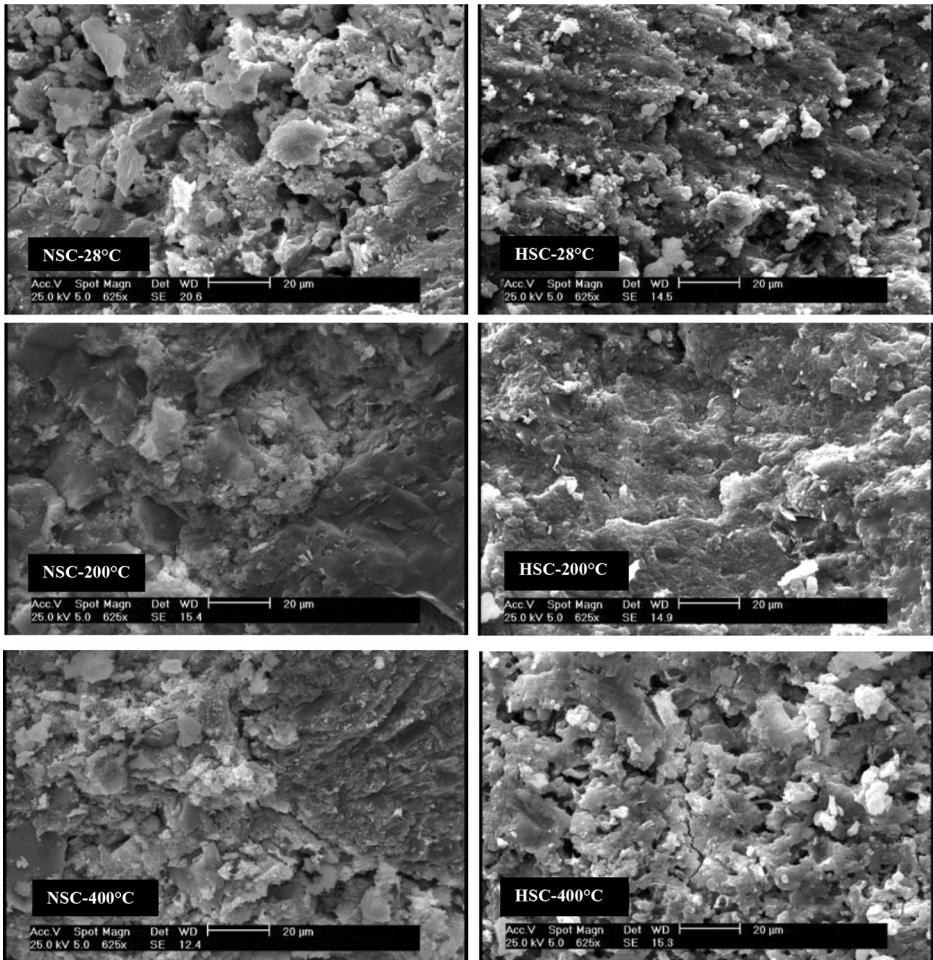


Figure 22. Microstructural transformation due to high temperatures exposure.

rienced higher temperatures. For instance, this value for HSC samples experienced 400 °C and 800 °C, was started from 700 °C and 610 °C.

3.3.2. Scanning Electronic Microscopy (SEM) Scanning Electronic Microscope methods can provide valuable insight into the microstructure's transformation of the cement matrix, especially at temperatures in which concrete show abnormal behavior. Because of that, the SEM test was performed on specimens exposed to 28, 200, and 400 °C. As can be observed from Fig. 22, high temperatures had detrimental effects on the porosity of concrete structure. In other words, those samples experienced lower temperatures had a denser structure. It should come as no surprise, the HSC had a more compact structure than NSC in room temperatures. At temperature 200 °C, there were no significant changes in the microstructure; however, a sort of voids stemmed from the evaporation of free water could be observed. At this temperature, the porosity of specimens (both in NSC and HSC) slightly increased, which was earlier noticed in the durability tests. Also, high temperatures resulted in delicate CSH crystals, leading to a reduction in density. When temperature exceeded 400 °C, the electronic microscope images showed more propagation of microcracks, along with an expansion in the existed ones. In other words, the number and extent of cracks increased, and segregated cracks formed an integrated network.

Although the mechanical deterioration of concrete is an indispensable part of high temperatures, HSC showed a better performance than NSC. The presence of silica fume caused a sort of pozzolanic reaction that culminated with secondary C-S-H gel. XRD results derived from previous study confirmed this fact [32]. This behavior diminished porosity, and ameliorated concrete strength, especially in HSC samples which had encompassed a higher amount of silica fume. Generally, silica fume in high strength concrete provides a higher amount of hydration products, together with a more compact structure. Because of that, it had a better performance in the durability and mechanical properties compared with NCS at low temperatures. It should be also mentioned that, in the range of 200–400 °C, a growth in mechanical properties was observed (almost in both types of concrete). This restrengthening, according to this study and previous investigations, can be attributed to the evaporation of inter-layer water and hardening of cement gel, which can result in van der waals forces between the cement paste layers [32, 52].

4. Conclusion

This investigation examined the mechanical and durability properties of the HSC and NSC at high temperatures, ranging from 28 °C to 800 °C, on 360 concrete specimens. Furthermore, a sort of equations to predict the mechanical behavior of HSC at high temperatures was proposed and compared with the previous studies. Finally, the microstructural analysis (including TGA and SEM) was used to gain a better understanding of microstructural behavior. Based on the test results, the following conclusions are drawn:

The initial compressive strength of concrete did not have a remarkable impact on the shear strength. In other words, the shear strength of the HSC was approximately 11% higher than NSC for reference specimens. However, as a result of deterioration in compressive strength and aggregate interlocking, it reduced to about 3% at 800 °C.

Although the proposed formula for mechanical properties had an acceptable agreement with the previous studies, in some cases, they were not capable of predicting accurately. Insufficient experimental data on tensile and shear strength of HSC at the hot condition, together with different testing conditions, can give rise to this disparity.

The HSC had better durability properties in low temperatures (below 400 °C) compared with the NSC. However, high-temperatures resulted in a severe microstructural deterioration in the HSC, degrading its durability to a greater extent.

Concerning microstructural transformation, the HSC had a higher amount of hydration products at high temperatures based on TGA graphs. Moreover, according to the SEM images, the extent of porosity in the HSC was higher than NSC at 400 °C, as opposed to lower temperatures.

5. Recommendation

There is a wide range of factors affecting the high-temperature behavior of concrete in the field condition. It should come as no surprise the experimental laboratory tests can fulfill a number of those, to a certain extent. For instance, heating rate, exposure time, durability tests, etc., can be widely varied in real-world problems. However, the invaluable results of this study, along with previous and future studies, together with employing novel and promising methods of data science on an extensive data set, can lead to a more reliable and realistic prediction for real-world problems. Hence it would add value to future studies a combination of previous experimental results with machine-learning frameworks.

Funding

This research did not receive any specific Grant from funding agencies in the public, commercial, or not-for-profit sectors.

Compliance with Ethical Standards

Conflict of interest The authors declared no potential conflicts of interest with respect to the research, authorship, and publication of this article.

References

1. Moghadam MA, Izadifard RA (2020) Effects of steel and glass fibers on mechanical and durability properties of concrete exposed to high temperatures. *Fire Saf J* 2020:102978
2. Eidan J, Rasoolan I, Rezaeian A, Poorveis D (2019) Residual mechanical properties of polypropylene fiber-reinforced concrete after heating. *Constr Build Mater* 198:195–206
3. Kodur V (2014) Properties of concrete at elevated temperatures. *Int Scholar Res Not* 2014:2014
4. Memon SA, Shah SFA, Khushnood RA, Baloch WL (2019) Durability of sustainable concrete subjected to elevated temperature—a review. *Constr Build Mater* 199:435–455
5. Toropovs N, Monte FL, Wyrzykowski M, Weber B, Sahmenko G, Vontobel P et al (2015) Real-time measurements of temperature, pressure and moisture profiles in high-performance concrete exposed to high temperatures during neutron radiography imaging. *Cem Concr Res* 68:166–173
6. Moghadam MA, Izadifard RA (2019) Experimental investigation on the effect of silica fume and zeolite on mechanical and durability properties of concrete at high temperatures. *SN Appl Sci* 1(7):682
7. Kodur VK (2018) Innovative strategies for enhancing fire performance of high-strength concrete structures. *Adv Struct Eng* 21(11):1723–1732
8. Caetano H, Ferreira G, Rodrigues JPC, Pimienta P (2019) Effect of the high temperatures on the microstructure and compressive strength of high strength fibre concretes. *Constr Build Mater* 199:717–736
9. Gyu-Yong K, Young-Sun K, Tae-Gyu L (2009) Mechanical properties of high-strength concrete subjected to high temperature by stressed test. *Trans Nonferrous Metals Soc China* 19:s128–s133
10. Behnood A, Ghandehari M (2009) Comparison of compressive and splitting tensile strength of high-strength concrete with and without polypropylene fibers heated to high temperatures. *Fire Saf J* 44(8):1015–1022
11. Chan Y, Peng G, Anson M (1999) Residual strength and pore structure of high-strength concrete and normal strength concrete after exposure to high temperatures. *Cement Concr Compos* 21(1):23–27
12. Khaliq W, Waheed F (2017) Mechanical response and spalling sensitivity of air entrained high-strength concrete at elevated temperatures. *Constr Build Mater* 150:747–757
13. Abaician R, Behbahani HP, Moslem SJ (2018) Effects of high temperatures on mechanical behavior of high strength concrete reinforced with high performance synthetic macro polypropylene (HPP) fibres. *Constr Build Mater* 165:631–638
14. Cülfik MS, Özturan T (2010) Mechanical properties of normal and high strength concretes subjected to high temperatures and using image analysis to detect bond deteriorations. *Constr Build Mater* 24(8):1486–1493
15. Chen B, Liu J (2004) Residual strength of hybrid-fiber-reinforced high-strength concrete after exposure to high temperatures. *Cem Concr Res* 34(6):1065–1069
16. Varona FB, Baeza FJ, Bru D, Ivorra S (2018) Influence of high temperature on the mechanical properties of hybrid fibre reinforced normal and high strength concrete. *Constr Build Mater* 159:73–82
17. Yusuf M (2019) Shear transfer strength of concrete after exposure to elevated temperature

18. Boulekbache B, Hamrat M, Chemrouk M, Amziane S (2012) Influence of yield stress and compressive strength on direct shear behaviour of steel fibre-reinforced concrete. *Constr Build Mater* 27(1):6–14
19. Gao D, Zhang L, Nokken M (2017) Mechanical behavior of recycled coarse aggregate concrete reinforced with steel fibers under direct shear. *Cem Concr Compos* 79:1–8
20. Moghadam MA, Izadifard R (2019) Evaluation of shear strength of plain and steel fibrous concrete at high temperatures. *Constr Build Mater* 215:207–216
21. Ahmad S, Bhargava P, Chourasia A, Sharma UK (2020) Shear transfer strength of uncracked concrete after elevated temperatures. *J Struct Eng* 146(7):04020133
22. Al-Owaisy SR (2007) Effect of high temperatures on shear transfer strength of concrete. *J Eng Sustain Dev* 11(1):92–103
23. Xiao J, Li Z, Li J (2014) Shear transfer across a crack in high-strength concrete after elevated temperatures. *Constr Build Mater* 71:472–483
24. Ma Q, Guo R, Zhao Z, Lin Z, He K (2015) Mechanical properties of concrete at high temperature—a review. *Constr Build Mater* 93:371–383
25. Bošnjak J, Ožbolt J, Hahn R (2013) Permeability measurement on high strength concrete without and with polypropylene fibers at elevated temperatures using a new test setup. *Cem Concr Res* 53:104–111
26. Mendes A, Sanjayan JG, Gates WP, Collins F (2012) The influence of water absorption and porosity on the deterioration of cement paste and concrete exposed to elevated temperatures, as in a fire event. *Cem Concr Compos* 34(9):1067–1074
27. ASTM C. 494 (1999) Standard specification for chemical admixtures for concrete. West Conshohocken, PA: ASTM International
28. Zarifian A, Izadi fard RA, Khalighi A, (2019) Experimental study on the behavior of thermally insulated RC beams strengthened with CFRP after their exposure to high temperatures compared to non-insulated ones. *Can J Civ Eng* 999:1–9
29. Standard B (2009) Testing hardened concrete. Compressive Strength of Test Specimens, BS EN, pp. 12390–12393
30. ASTM C. 496/C 496M-04 (2004) Standard test method for splitting tensile strength of cylindrical concrete specimens 4:5
31. J.S. of C. Engineering J-S. Method of Test for Shear Strength of Steel Fiber Reinforced Concrete (SFRC). Tokyo1990
32. Moghadam MA, Izadifard RA (2020) Effects of zeolite and silica fume substitution on the microstructure and mechanical properties of mortar at high temperatures. *Constr Build Mater* 2020:119206
33. Drzymala T, Jackiewicz-Rek W, Gałaj J, Śukys R (2018) Assessment of mechanical properties of high strength concrete (HSC) after exposure to high temperature. *J Civ Eng Manag* 24(2):138–144
34. Husem M (2006) The effects of high temperature on compressive and flexural strengths of ordinary and high-performance concrete. *Fire Saf J* 41(2):155–163
35. Eurocode B (2004) 2: Design of concrete structures-part 1–2: general rules-structural fire design. European Concrete Platform, Brussels
36. H.S. Müller HKH (1990) Evaluation of the time dependent behavior of concrete. CEB Com Euro 429 Int Du Béton, Bull
37. Thomas J, Ramaswamy A (2007) Mechanical properties of steel fiber-reinforced concrete. *J Mater Civ Eng* 19(5):385–392
38. AC, editor State-of-the-art Report on High-strength Concrete (ACI 363R-84)1984: American Concrete Institute
39. Xu B, Shi H (2009) Correlations among mechanical properties of steel fiber reinforced concrete. *Constr Build Mater* 23(12):3468–3474

40. Committee A, editor Building code requirements for structural concrete (ACI 318–05) and commentary (ACI 318R-05)2005: American Concrete Institute
41. Ramadoss P (2014) Combined effect of silica fume and steel fiber on the splitting tensile strength of high-strength concrete. *Int J Civ Eng* 12(1):96–103
42. Wafa FF, Ashour SA (1992) Mechanical properties of high-strength fiber reinforced concrete. *Mater J* 89(5):449–455
43. Perumal R (2015) Correlation of compressive strength and other engineering properties of high-performance steel fiber–reinforced concrete. *J Mater Civ Eng* 27(1):04014114
44. Rashid M, Mansur M, Paramasivam P (2002) Correlations between mechanical properties of high-strength concrete. *J Mater Civ Eng* 14(3):230–238
45. Smith HK, Reid E, Beatty AA, Stratford TJ, Bisby LA (2011) Shear strength of concrete at elevated temperature. In: International conference on applications of structural fire engineering
46. Mansur M, Vinayagam T, Tan K-H (2008) Shear transfer across a crack in reinforced high-strength concrete. *J Mater Civ Eng* 20(4):294–302
47. Khaloo AR, Kim N (1997) Influence of concrete and fiber characteristics on behavior of steel fiber reinforced concrete under direct shear. *Mater J* 94(6):592–601
48. Khanlou A, MacRae G, Scott A, Hicks S, Clifton G, editors (2012) Shear performance of steel fibre-reinforced concrete. Australasian Structural Engineering Conference 2012: The past, present and future of Structural Engineering; 2012: Engineers Australia
49. BSI. BS EN 1992-1-1: 2004+ A1: 2014: Eurocode 2: Design of concrete structures. General rules and rules for buildings. BSI London, UK; 2004
50. ASTM C (2012) Standard test method for electrical indication of concrete’s ability to resist chloride ion penetration. C1202–18. 2012
51. Rahmani T, Kiani B, Sami F, Fard BN, Farnam Y, Shekarchizadeh M, editors (2011) durability of glass, polypropylene and steel fiber reinforced concrete. in: proceedings of the international conference on durability of building materials and components, Porto, Portugal
52. Castillo C (1987) Effect of transient high temperature on high-strength concrete

Publisher’s Note Springer Nature remains neutral with regard to jurisdictional claims in published maps and institutional affiliations.